IMPROVEMENT OF STRENGTH OF LOW CARBONST 37 STEEL BY GROOVE PRESSING

Hamdi Abdulhamid Raghs
Faculty of engineering, Omar Al Mukhtar University, Libya,
E- mail: hamdi.raghs@omu.edu.ly, hamdiraghis@yahoo.com

الملخص

ضغط الأخدود المقيد (**CGP**) هو تقنية حديثة لتطوير هياكل الحبوب متناهية الصغر في الصفائح المعدنية للحصول على خصائص مواد فائقة. في **CGP** ، تخضع عينات الصفائح المعدنية للتمويج المتكرروالاستقامة تحت حالة تشوه من خلال استخدام الضغط البديل مع القوالب المحززة. يؤدي هذا إلى إحداث قدر كبير من الإجهاد في عينة الصفائح المعدنية دون تغيير أبعادها الأولية. ضغط الأخدود المقيد هو طريقة تشوه لدن شديدة يتم تطبيقها لزيادة متانة المعادن وزيادة الصلابة.

يدرس هذا البحث تغيرالخواص الميكانيكية لصفيحة الفولاذ **St 37** نتيجة التشوه اللدونة المفرط-بسبب ضغط الأخدود ، والذي يتم من خلال تطبيق قوى ضغط عالية على صفيحة الفولاذ . بعد عملية ضغط الأخدود تم إجراء قياسات الصلابة للفولاذ **St 37** ولوحظ زيادة في قيم المتانة. وكذلك وجدنا في صور المجهر الإلكتروني (**SEM**) وصور حيود التشتت الإلكتروني (**EBSD**) المأخوذة من المقطع العرضي للفولاذ وجود تشوه لدن شديد, وبالتالي لوحظ وجود هياكل دقيقة الحبيبات على السطح وتحت السطح مباشرة . سيتم الضغط على الفولاذ الكربوني المنخفض **St37** عن طريق ضغط أخدود محدود في طرق مختلفة في درجة حرارة الغرفة وسنحاول قياس تأثير مقدار التشوه. سيتم فحص المواد المشوهة بشكل مجهري باستخدام تضاريس السطح. بالإضافة إلى ذلك ، سيتم فحص الخواص الميكانيكية وتغيرات الصلابة بأستخدام أختبار الشد وقياسات الصلابة في أجزاء مختلفة من الفولاذ.

الهدف من هذا البحث هو الكشف عن التغيرات في الخواص الهيكلية الدقيقة للفولاذ **St 37** لتحسين الطابع الميكانيكي لضغط الأخدود المحدود لتكون النتائج مرتبطة

بخصائص البنية المجهرية. في سياق الاختبارات الميكانيكية ، ستتم مقارنة سلوك مادة الفولاذ منخفض الكربون **St37** .

Abstract

Constrained Groove Pressing (CGP) is an extreme plastic deformation method applied to increase the strength of metals. Restricted groove pressing is a process that causes both an increase in strength and an increase in hardness in metals. This study covers the existence of fine-grained structures and the change of mechanical properties in materials as a result of excessive plastic deformation of metallic materials together with the grooved press, which is limited by applying high pressing forces. After the process, hardness measurements of St 37 steel materials were made and an increase in strength and hardness values was observed. On other hand, in Scanning Electron Microscopy images (SEM), and Electron Backscatter Diffraction images (EBSD) which taken from the cross-section of the metals, the presence of severe plastic deformation, and consequently fine-grained structures was observed on the surface and just below the surface. St37 low carbon steel will be deformed by limited groove pressing, in different routes at room temperature and the effect of the amount of deformation will be tried to be measured. Deformed materials will be microstructurally examined using surface topography. In addition, mechanical properties and hardness changes in different parts of the material will be examined.

The objective of this research is to clearly reveal the effect-relationships and correlations of the changes in the microstructural properties of the material on the improvement of the mechanical character of the limited groove pressing, which is applied as an extreme plastic deformation method. In the context of mechanical tests, the behaviour of St 37 low carbon steel material, which is plastically deformed under both single and cyclic loads, will be compared with the conventionally produced one and the results will be tried to be correlated with the microstructure properties.

Key Words: St 37 steel, Constrained groove pressing (CGP), severe plastic deformation (SPD), Electron Backscatter Diffraction

(EBSD), Scanning Electron Microscopy (SEM), (CAM) Computer Aided Manufacturing.

1. Introduction

Compared to coarse-grained materials, materials with ultra-fine-grained or nano-structured properties are an important subject to investigate today. One of the important reasons for this is the display of super-plastic behavior, which is one of the advanced mechanical properties. In addition, it is important to use nano-granular materials in many industries such as automotive, space and aircraft, defense, energy and biomedical [1,2,3].

The production of materials with nano-granular structure in terms of volume is carried out by both inductive and deductive methods. Inductive methods generally involve combining fine-grained powder particles with different applications. However, only deductive methods use severe plastic deformation. The formation of nanocrystallographic structure as a result of severe plastic deformation is associated with dislocation cells that occur together with plastic deformation [4,5,6].

This study aimed to establish a qualitative correlation between material microstructure and mechanical properties. The main achievement of the research is that the application is low cost compared to others in terms of cost and that it can be easily applied in existing areas where the goal of only mechanical and physical change without chemical reaction and chemically changing the microstructure of the material will expand the application areas, and there have been many studies lately in this field [7,8].

2. Material and methods

2.1. Experimental materials

In this study, special mold manufacturing that can create severe plastic deformation has been carried out, and the dimensions of mold are 200 x150 x 100 mm. The bottom mold to be manufactured has been completed with the help of the necessary Solidworks 2016 package program (Figure 1). Low alloy steel was preferred as the mold material, low alloy steel material which can be easily processed, heat treated (quenched and tempered).The design and manufacture of mold used in the processes was carried out within the scope of the research.

The chemical composition of St 37 steel is given in Table 1. It is aimed to be pressed in the form of 1 pass (stage), 2 passes and 4 passes, and These passes mean the stages of pressure on the metal sheet, and the dimensions of sheet plate are 160 x 100 mm, and the sheet were of 2 mm thickness.

Table 1. Chemical composition (%) of St37 low carbon steel

	C	Mn	Si	Ni	P	S
% Weight (min.)	0,10	0,20	0,40	0,00	0,040	0,050
% Weight (max.)	0,17	0,50				

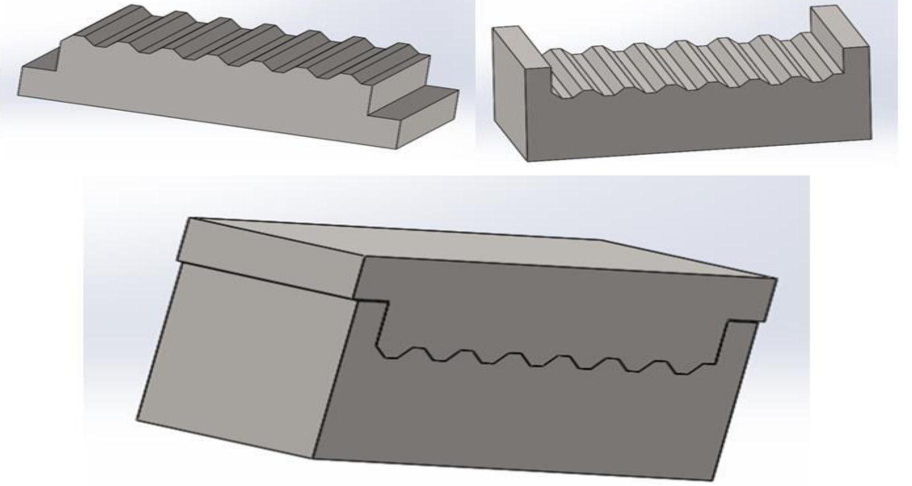

Fig. 1. Solidworks drawings of the mold used in experimental studies

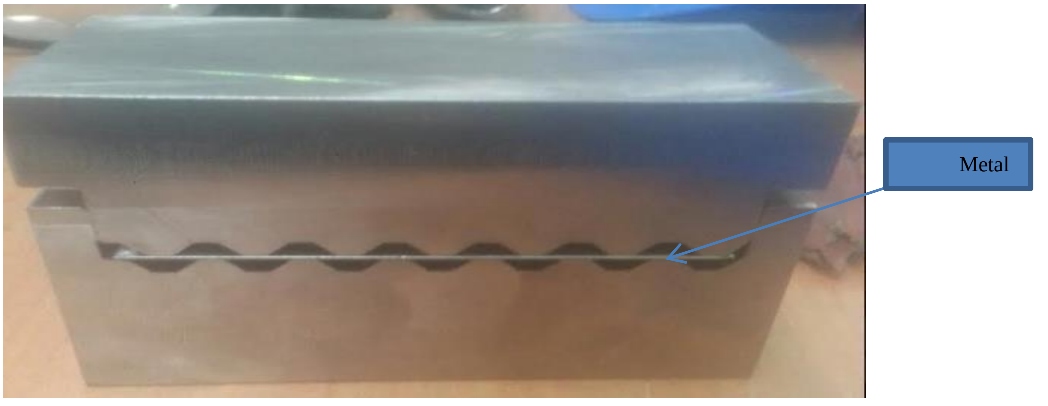

Fig. 2. The mold used in experimental studies and the appearance of the sheet plate placed in the mold

After the completed mold of the design (low alloy steel material) was programmed in the Master CAM processing package program (Dimensions of mold are 200 x150 x 100 mm,), it was processed in CNC milling. For limited groove pressing, 1 mm and 2 mm (Depth of pass in mm), sheet St 37 were used and pressed in the form of 1 pass, 2 passes and 4 passes (Figure 2).

Microstructural investigations and tests were carried out together in order to determine the change of mechanical properties after the limited groove pressing of the samples. The tests performed in order to determine grain size change and morphology differences are as follows:

2.2. Electron Backscatter Diffraction (EBSD):

It is a test performed to determine the formation and appearance of the obtained ultra-fine particles, crystallographic orientations and the change of fine-grained layer thickness according to the applied extreme plastic deformation. Electron backscatter diffraction (EBSD) microscopy is a characterization technique used with scanning electron microscopes (SEM) for determination of crystallographic information present in both metal samples.

Much like energy dispersive X-ray spectroscopy (EDS), which provides the elemental composition through the interaction of electron beam and individual atoms, EBSD uses the interaction of the electron beam with a localized, periodic arrangement of atoms to generate diffraction patterns that can be captured with an unique camera-beam-detector geometry.

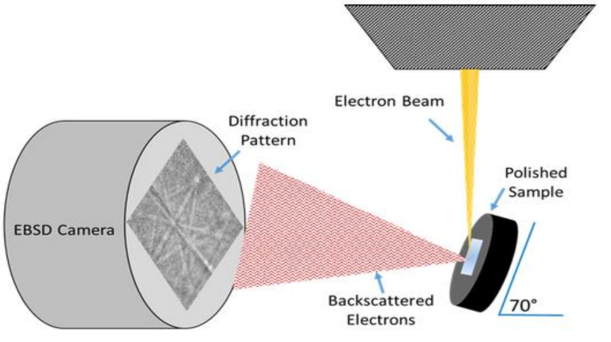

Fig. 3. Illustration of the EBSD detection geometry and a conventional detector

2.3. Optical microscope (OM):

Microstructure investigations of St37-2 steel used in the experiments were made using Nikon SMZ745T model optical microscope The optical microscope has a 0.67-5X zoom magnification and a working distance of 115mm. With the use of extra optical lenses, it can magnify up to 3.35-300X. Optical microscope has a millimeter table with a sensitivity of 0.01 mm, which can move in the X and Y directions. The changes that occur in ST37-2 are transferred to the computer environment with a camera placed on the microscope and these images can be examined and analyzed by using the Clemex Captiva 6.0 computer software (Figure 4).

Fig. 4. Optical microscope (Nikon SMZ745T)

2.4. Scanning Electron Microscopy (SEM)

Scanning electron microscopy can perform imaging analysis of structures in the material at the micro and nano level. In addition, qualitative and quantitative elemental analysis can be performed within the sample, the distribution of elements can be monitored with the mapping technique, and phase analysis can be performed using the EBSD technique. With this test, it is aimed to determine the formation and appearance of ultra-fine grains, crystallographic orientations and the variation of fine-grained layer thickness according to the applied extreme plastic deformation. The test was carried out with a TESCAN MAIA3 XMU model device.

Fig. 5. Scanning Electron Microscopy (SEM)

2.5. Microhardness

In the experimental studies, the Brinell measurement method was chosen by using the Qness Q250M hardness device, which is given in (Figure6). HV0.01 was applied as a load for hardness measurement. The samples are prepared in accordance with TS EN ISO 6506 standards and have dimensions of 50x50x10 mm. The hardness values were taken as the average of three applications.

Fig. 6. Qness Q250M brand hardness device

2.6. Tensile Test

Produced composite samples were pulled at a tensile speed of 1 mm/min in SHIMADZU AG-IS brand 50 kN capacity tensile test device. After the test, the stress-strain diagrams, tensile strength, yield strength and elongation values of the samples were obtained automatically from the computer-controlled TRAPEZIUM program (Figure 7), the samples produced from material were subjected to the tensile test after process of constrained groove pressing, in order to detect the changes in properties of material. .

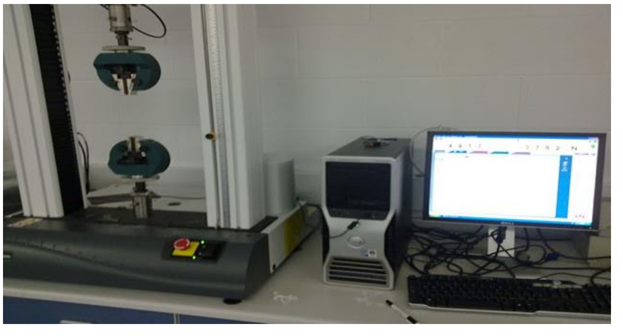

Fig. 7. Tensile Test machine

2.7. Constrained groove pressing (CGP)

The bottom mold to be manufactured has been completed with the help of Solidworks program (Figure 8). After the completed mold of the design was programmed in CAM software, it was processed in CNC milling. For constrained groove pressing, 1 mm and 2 mm (Depth of pass in mm) sheet metal were used. To determine the change of mechanical properties after the constrained groove pressing of the samples (dimensions of sheet plate are 160 x 100 mm), microstructural investigations and tests were carried out.

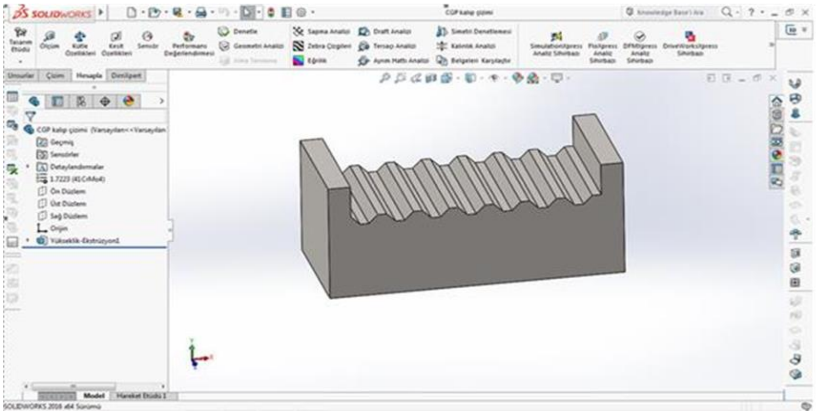

Fig. 8. Pressing lower die with limited groove

3. Results and Discussion

3.1. Microstructural studies

SEM-EBSD analyzes applied to the sample taken from the pressed material as a result of pressing the St37 low carbon steel used in the experimental studies in a grooved mold were examined, figure 9 shows EBSD images of the specimens with constrained groove pressing applied in different passes (These passes mean the stages of pressure on the metal sheet). The macro changes in the surfaces of the samples, analyzes of the microstructure are given in next figure. Tool traces after process are shown in Figures 9.a, 9.b, 9.c and 9.d, the presence of movement traces of process of (CGP) is remarkable. It was observed that the presence of movement traces of processes was more pronounced with the increase in the depth of the pass. Images of 1st Pass, 2nd Pass, 3rd Pass, 4th Pass procedures are shown in figure. After the process, a change in the grain structure was observed after a plastic deformation effect on the surface area. The structure affected by the process on the surface was printed more compared to the interior and the homogeneity of the structure deteriorated. It was noted that the striking distributions in the interior structure intertwined and the distinctive structures began to disappear. At the same time, the thickness of the deformed region increased with the increase of the effect of process. It is seen that the grains are oriented from left side to right side after process of (CGP) at 2, 3, and4 intensity, which also indicates the CGP direction. Although process-induced deformation is observed in the surface line, it has been observed that the effect is more limited than pressing or surface mechanical deformation process.

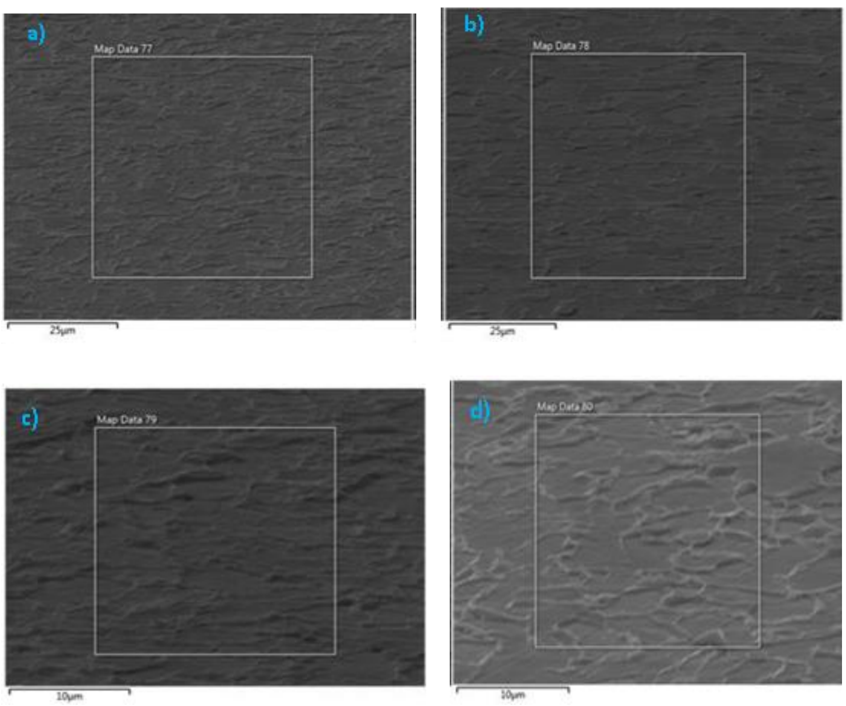

Fig. 9. Electron images taken for each pass at the beginning of the experiment a) 1st Pass, b) 2nd Pass, c) 3rd Pass, d) 4th Pass

Voltage, angle, data rate parameters used in EBSD studies to obtain the necessary images are given in Table 2, Table 3, Table 4 and Table 5 for 1st Pass, 2nd Pass, 3rd Pass, 4th Pass, respectively.

Table 2. 1st Pass EBSD analysis conditions of ST37-2 Steel

Accelerating Voltage	**20.00 kV**
Specimen Tilt (degrees)	**70.00 °**
Hit Rate	**78.89%**
Speed of Acquisition	**40.13 Hz**

Table 3. 2nd Pass EBSD analysis conditions of ST37-2 Steel

Accelerating Voltage	20.00 kV
Specimen Tilt (degrees)	70.00 °
Hit Rate	84.89 %
Speed of Acquisition	40.13 Hz

Table 4. 3rd Pass EBSD analysis conditions of ST37-2 Steel

Accelerating Voltage	20.00 kV
Specimen Tilt (degrees)	70.00 °
Hit Rate	70.81 %
Speed of Acquisition	40.23 Hz

Table 5. 4th Pass EBSD analysis conditions of ST37-2 Steel

Accelerating Voltage	20.00 kV
Specimen Tilt (degrees)	70.00 °
Hit Rate	77.38 %
Speed of Acquisition	40.23 Hz

Elemental analysis results obtained in preliminary scans performed for the purpose of coloring elemental analysis and distribution in EBSD analysis are shown in Table 6.

Table 6. Phase acquisition for ST37-2 steel

Phase	a	b	c	Alfa	Beta	Gamma	Space Group	Database
Iron	2.89 Å	2.89 Å	2.89 Å	90.00 °	90.00 °	90.00 °	229	ICSD
C	4.28 Å	4.28 Å	4.28 Å	90.00 °	90.00 °	90.00 °	206	ICSD
Fe3C	5.11 Å	6.78 Å	4.54 Å	90.00 °	90.00 °	90.00 °	62	HKL
C	3.54 Å	3.54 Å	3.54 Å	90.00 °	90.00 °	90.00 °	216	ICSD
P	3.31 Å	10.29 Å	4.30 Å	90.00 °	90.00 °	90.00 °	64	ICSD
P	2.38 Å	2.38 Å	2.38 Å	90.00 °	90.00 °	90.00 °	221	ICSD
P	3.38 Å	3.38 Å	8.81 Å	90.00 °	90.00 °	120.00 °	166	ICSD
P	9.21 Å	9.15 Å	22.60 Å	90.00 °	106.10 °	90.00 °	13	ICSD
S	7.09 Å	7.09 Å	4.30 Å	90.00 °	90.00 °	120.00 °	154	ICSD
S	17.60 Å	9.25 Å	13.80 Å	90.00 °	113.00 °	90.00 °	3	ICSD

In Figure 10, the regions to be examined in images analysis were determined, and the analysis and scanning was carried out by introducing the elements and compounds to be scanned to the system. The compounds formed by the iron-based internal structure and alloying elements in the microstructure attract attention. In images analysis, the deformed structure in general was distinguished from the internal structure as oriented. It was also seen in the images analysis that the layer thicknesses affected by the deformation increased as the processing intensity increased. This situation, in which the surface integrity and flatness is largely preserved after applications, shows that the process can be an important surface extreme plastic deformation method.

Considering the measurement scales in the images obtained in Figure 11, grain size thinning due to dislocation movements is encountered. Especially in the 3rd pass, the presence of sub-grains with dislocation density in the grains draws attention. It is noteworthy that the grain size is considerably finer, especially when it is untreated and subjected to single pass process.

However, as the processing conditions get heavier, the effect on the surface gets heavier, the deformation effective layer thickness deepens considerably and it is thought that it may have an effect in terms of mechanical properties. Unlike the optical images, it showed the presence of a nebula structure on the surface with limited detailed characterization. Studies in the literature have shown that this structure is a deformed ultra-fine-grained or Nano crystalline structure.

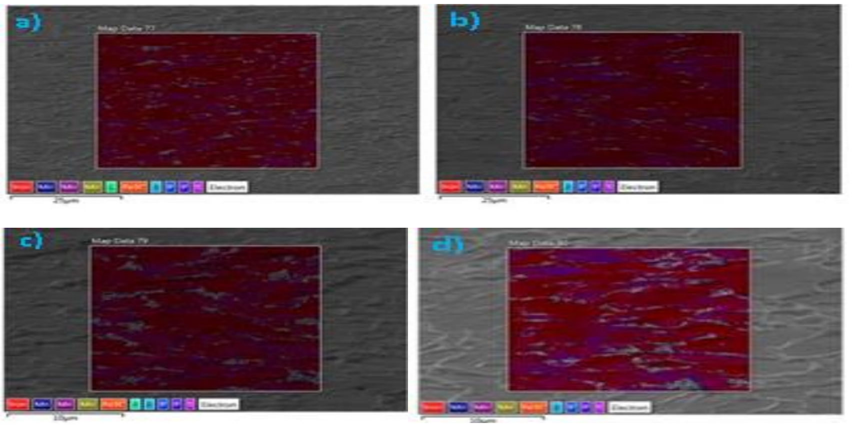

Fig. 10. Images of electron back reflection diffraction test result
a) 1st Pass, b) 2nd Pass, c) 3rd Pass, d) 4th Pass

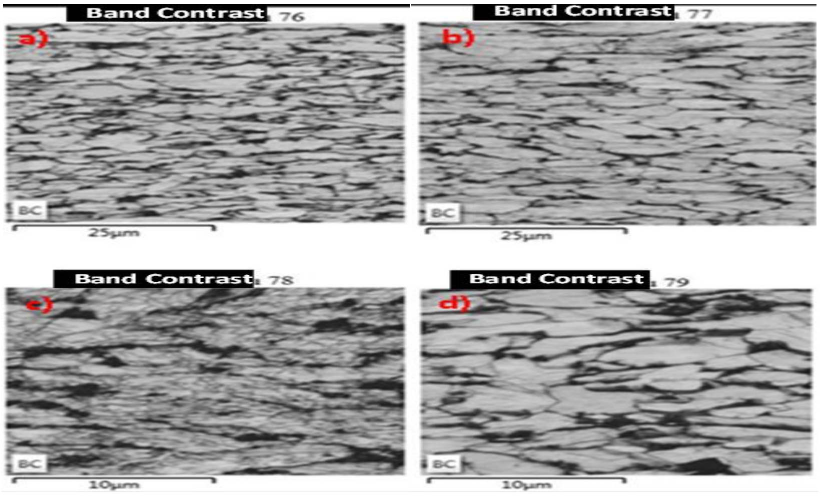

Fig. 11. Band contrast images as a result of electron back reflection diffraction test a) 1st Pass, b) 2nd Pass, c) 3rd Pass, d) 4th Pass

In Figure 12, As a result of EBSD analysis, the nanostructured region was determined prominently in 2nd Pass,, while the nanostructured and fine-grained region was determined together prominently in 3rd Pass, 4th Pass. As the effect of plastic deformation in the processes is increased, there is an increase in the layer thickness affected by the processes, it was observed that treatments largely preserved the surface integrity and flatness, and no oxide layer and surface cracks were observed after the treatments.

Due to the heterogeneous structure of the gradient materials with the surface deformations, significant increases in both strength and ductility properties have begun to be observed. It is thought that this situation will have a significant impact on the new type of material and the ductility-strength relationship. After the EBSD analysis, different structures draw attention from the surface to the interior in general terms. Similar approaches are emphasized in gradient materials, which have just begun to be introduced in the literature.

As seen in Figure 13, a nanocrystalline structure was obtained in a very thin layer. Due to the low impact, the layer affected by any deformation in the lower part does not attract attention, and it was concluded that the thickness of the two layers is very close to each other. The reason for this is thought to be the increase in the distance between these two layer thickness boundaries with the increase in intensity. It was observed that the thickness of both nanocrystalline and deformation-affected, oriented fine-grained layers increased significantly as the processing conditions increased, analysis of was performed to determine the phase change, grain size change and layer differences of such structures.

Different structures emerged in examination after 1st Pass, 2nd Pass, 3rd Pass, 4th Pass procedures. In the outermost layer, which is faced with a large proportion of the deformation energy at the surface and below, the presence of main layers: nanocrystalline (ultra-fine) grained layer, fine-grained, deformation-affected layer where the deformation effect gradually decreases but the effect is palpable, and coarse-grained structure that is not affected by the process.

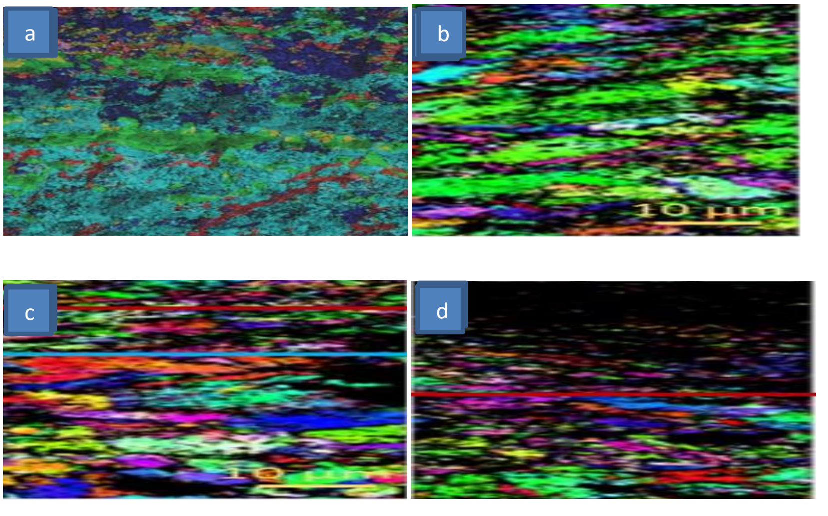

Fig. 12. EBSD images from the cross-sectional region of samples

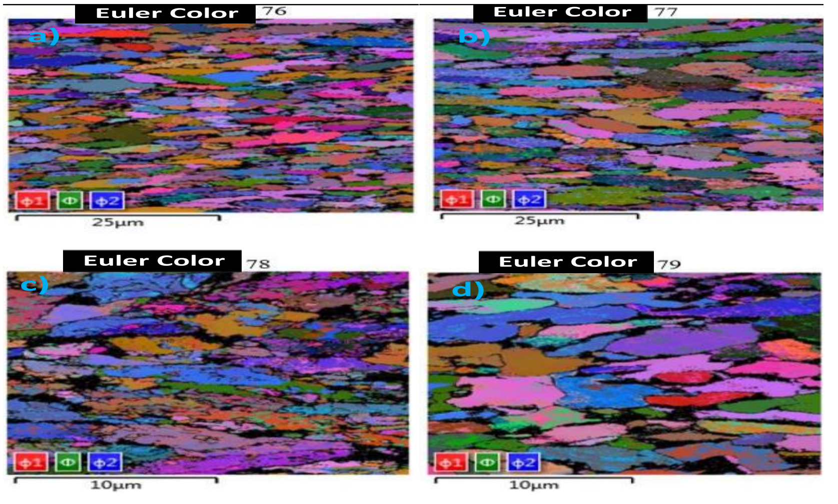

Fig. 13. Euler color images as a result of electron back reflection diffraction test a) 1st Pass, b) 2nd Pass, c) 3rd Pass, d) 4th Pass

3.2. Microhardness Results

The graph of the hardness measurements obtained as a result of pressing the St37 low carbon steel used in the experimental studies in the grooved mold is given in Figure 14.

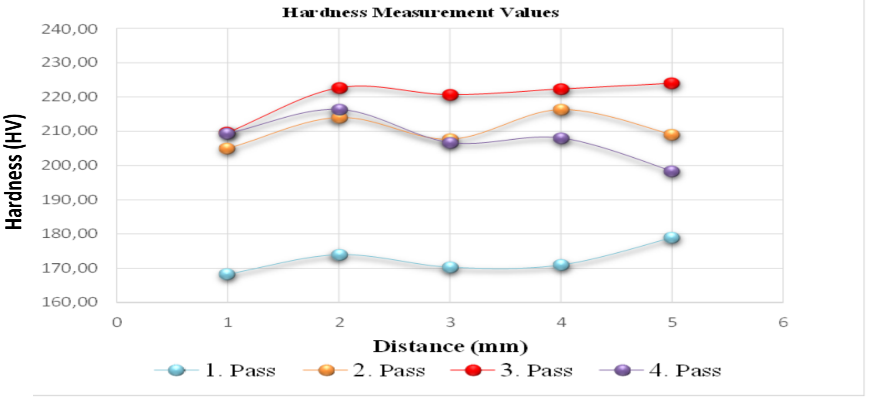

Fig. 14. Graph of hardness measurements

By examining the hardness measurement values given in Figure 14, it was observed that the hardness values increased in the first 3 passes. In this case, they support each other with grain refinements.

Hardness values were generally obtained at the highest levels in the 3rd pass, where the grain thinning was most intense. Plastic deformation by compressive loading on the surface of the material creates a localized cold-worked zone on the sample surface. This formed region hardens with the effect of plastic deformation. By increasing the effect of plastic deformation, the layer thickness of the formed layer increases. This hardened layer also provides positive contributions to the improvement of corrosion resistance and wear resistance values.

The increase in the thickness of the layer affected by plastic deformation, where the processes have a positive effect in terms of effect on the hardness.

3.3. Tensile test results and evaluation

In the lab, the CorelDraw software was employed to make a drawing of specimens from the sheet plate for tensile testing. These were carried out to reveal certain mechanical characteristics. Figure 15 show the specimen from sheet metal, the initial results point to the stress and strain curve as well as the mechanical properties of the specimens for sheet metal.

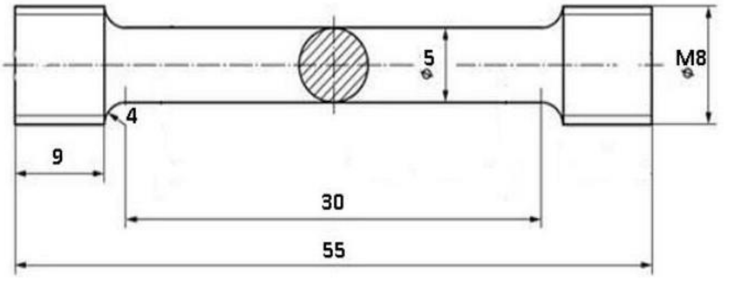

Fig. 15. Tensile test samples dimensions

The samples produced from steel material were subjected to the tensile test in order to detect the changes in the mechanical properties of the material after process of (CGP). After the test, the stress-strain graph, tensile strength, yield strength and elongation data of the samples were obtained, images of the samples obtained are given in Figure 16.

Fig. 16. Tensile test samples in the lab

Figure 17 shows the stress-strain graph obtained from the tensile test applied to the samples, and the strength-ductility values are given in Table 7.

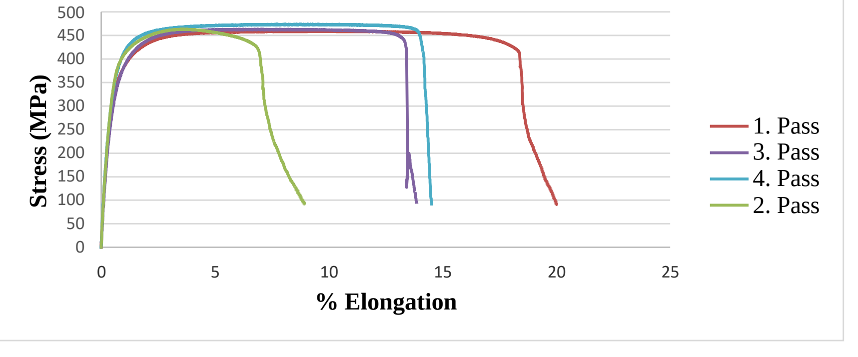

Fig. 17. Tensile test chart of samples

When the stress-strain graphs (Figure17) are examined, significant reductions in percent elongation have occurred after pressing with limited grooves that cause severe plastic deformation. A significant increase was observed in yield and tensile strengths with the increase in the amount of passes. It was noteworthy that the percent elongation was below a significant level as the deformation was very effective in the 3rd pass. A remarkable decrease was observed especially in yield strength due to insufficient ductility. From table7, we can see a difference in the elongation values of samples, because the elongation determines the stress-strain changes up to the point of the yield stress of material (elastic region), and elongation at yield is related to the ability of specimen to resist changes of shape before it deforms irreversibly. Also, elongation is inversely proportional to Young's modulus at each point.

The morphological behavior of rupture during tensile offers a specific approach to understanding the ductility and strength properties of samples. It has been observed that the outer surface undergoing plastic deformation shows the necking phenomenon compared to the inner surface. According to the tensile test results, it was observed that process applied increased the strength and ductility properties together, and it provides positive contributions to the mechanical properties of the material. This situation has been shown both in this study and in other literature studies, which eliminate the strength-ductility balance construct by surface extreme plastic deformation applications and gradient materials.

Table 7. Tensile test results

Pass Number	yield strength (MPa)	Max tensile strength (MPa)	Elongation %
1	286,352	459,2	20,03
2	315,374	463,6	8,92
3	259,350	463,3	13,86
4	311,261	474,4	14,53

4. Conclusion

The results obtained as a result of experimental studies are given below:

- When measuring scales are taken into account in EBSD images, grain size thinning due to dislocation movements is encountered.
- The grain size is considerably finer in the other passes than in the untreated and single-pass process.
- As a result of the hardness measurement values, it was concluded that the hardness values increased in the first 3 passes.

- Grain refinements were most intense in the third pass.
- The hardness values were obtained at the highest levels in the 3rd pass.
- Significant reductions in percent elongation have occurred after pressing with limited grooves, which creates severe and excessive plastic deformation.
- Due to the inability to create sufficient ductility in the 3rd pass compared to the other passes, a remarkable decrease was observed especially in the yield strength.

4.1. Recommendations

- In line with the results obtained, the test results could not be interpreted with definite expressions. Therefore, the number of passes can be increased.
- In order to increase the number of passes, it is possible to increase the force in the used press by examining the mold material again.

5. Acknowledgements

The author would like to take this opportunity to thank a number of individuals who have in one way or another made the production of this research possible. I thank all of technicians at Duzce University, Bartin University, and Karabuk University for all the help and guidance throughout my research, whether it was with lab equipment or procedures, or just research questions and discussions, you have all been of great support.

6. References

[1] Unal, O., and Varol, R., "Almen İntensity Effect on Microstructure and Mechanical properties of Low Carbon Steel Subjected to Severe Shot Peening", Applied Surface Science, 290: 40-47 (2014).
[2] Olugbade, T.O. and Lu, J., "Literature Review on the Mechanical Properties of Materials After Surface Mechanical Attrition Treatment (SMAT)", Nano Materials Science, 2:3-31 (2020).
[3] Revankar, G.D., Shetty, R., Rao, S.S., and Gaitonde, V.N., "Analysis of Surface Roughness and Hardness in Ball Burnishing of Titanium Alloy", Measurement, 58:256-268 (2014).

[4] Mohamed, A.O., Farhat, Z., Warkentin, A., and Gillis, J., "Effect of a Moving automated Shot Peening and Peening Parameters on Surface Integrity of Low Carbon Steel", Journal of Materials Processing Tech., 277: 116399 (2020).
[5] Buldum, B.B., Cagan, S.C., "Study of Ball Bunishing Process on the Surface Roughness and Microhardness of AZ91D Alloy", Experimental Techniques, 42:233-241 (2018).
[6] Maleki, E., Unal, O. and Kashyzadeh, K.R., "Surface Layer Nanocrystallization of Carbon Steels Subjected to Severe Shot Peening: Analysis and Optimization", Materials Characterization, 157:109877 (2019).
[7] Pan, Q. and Lu, L., "Improved Fatigue Resistance of Gradient Nanograined Metallic Materials: Suppress Strain Localization and Damage Accumulation", Scripta Materialia, 187:301-306 (2020).
[8] Maleki, E. and Unal, O.,"Roles of Surface Coverage Increase and Re-peening on Properties of AISI 1045 Carbon Steel in Conventional and Severe Shot Peening Proceses", Surfaces and Interfaces, 11:82-90 (2018).
[9] Science Direct, "From: Metallic Biomaterials Processing and Medical Device Manufacturing", https://www.sciencedirect.com/topics/materials-science /electron-backscatter-diffraction (2022).
[10] Geochemical Instrumentation and Analysis ,"Electron Backscatter Diffraction(EBSD)",https://serc.carleton.edu/research_education/geochemsheets/ebsd.html
[11] Nikon Metrology, "microscopes with powerful image resolving capabilities and all for a reasonable price.", https:// www. Nikon me trology.com/en-us/industrial-microscopes/stereo-microscopes-smz745-745t
[12] Nikon , "Nikon's stereoscopic microscope with 7.5x zoom and 115 mm working distance - a superior model in this category.",https://www.nikon.com/products/industrial-metrology/lineup/microscopestereoscopic_microscopes/ smz745_745t/

[13] TESCAN, “TESCAN SEM Solutions”, https://www.tescan.com/ product- portfolio/sem/

[14] Cardiff Catalysis, “MAIA-3 Field Emission Gun Scanning ElectronMicroscope(FEG-SEM”, https:// www. cardiff.ac.uk/cardiff-catalysis-institute-electron-microscope-facility /facilities/tescan-maia-3-field-emission-gun-scanning-electron-microscope-feg-sem.

[15] Qatm-quality assured,“materialography&hardness testing”, https://www.qatm.com/?gclid=eaiaiqobchmi9cscnltd-qivtoxocr3u3qryeaay asaaegij2vd_bwe.

[16] Environmental XPRT,“Qness-ModelQ250-Micro Hardness Tester”,https://www.Environmental –expert .com/ products /qness- model-q250-micro-hardness-tester-657050.

[17] TESTEX,“TensileTester”,https://www.testextextile.com/ producttensiletester/?gclid=EAIaIQobChMInuXov7fd-QIVh53VCh1rywq HE AAYAy AAEgK88PD_BwE.

[18] shimadzu, “Tensile Test System” ,https: //www .shimadzu .com/an / test/ tmc/find/material/00/6/1/957

[19] Estrin, Y. and Vinogradov, A., “Extreme Grain Refinement by Severe Plastic Deformation: A Wealth of Challenging Science”, Sciverse Sciencedirect, 61:782-817 (2013).

[20] Bourebia, M., Bouri, A.,Gharbi, A., Ghelloud, O. and Bouhamla, K., “Study of the Effect Burnishing on Superficial Hardness and hardening of S355JR Steel Using Experimental Planning”, Sciencedirect, 157:568-577 (2019).

[21] Zrnik, J., Dobatkin, S. V. ve Mamuzi, I., “Processing of metals by severe plastic deformation(Spd) ”, Structure And Mechanical Properties Respond, 47(3): 211-216 (2008).

[22] Todaka,Y.,Umemoto,M.veTsuchiya,K.,“Nano crystallization in carbon steels by various severe plastic deformation processes”, *Reviews ofAdvanced.Materials Science,* 409-416 (2005).

[23] Pippan, R., Wetscher, F., Hafok, M., Vorhauer, A. ve Sabirov, I., “The limits of refinement by severe plastic deformation”, *Advanced Engineering Materials*, 1047-1056 (2006).